

# Cyanide-Bridged Mn(III)–Fe(III) Bimetallic Complexes Based on the Pentacyano(1-methylimidazole)ferrate(III) Building Block: Structure and Magnetic Characterizations

Wei-Wei Ni, Zhong-Hai Ni, Ai-Li Cui, Xin Liang, and Hui-Zhong Kou\*

Department of Chemistry, Tsinghua University, Beijing 100084, P. R. China

Received April 5, 2006

Seven cyanide-bridged bimetallic complexes have been synthesized by the reaction of  $[\text{Fe}(\text{1-CH}_3\text{im})(\text{CN})_5]^{2-}$  with Mn(III) Schiff base complexes. Their crystal structure and magnetic properties have been characterized. Five complexes,  $[\text{Mn}_2(\text{5-Brsalen})_2\text{Fe}(\text{CN})_5(\text{1-CH}_3\text{im})\cdot\text{H}_2\text{O}$  (**1**),  $[\text{Mn}_2(\text{5-Clsalen})(\text{H}_2\text{O})_2\text{Fe}(\text{CN})_5(\text{1-CH}_3\text{im})\cdot\text{H}_2\text{O}$  (**2**),  $[\text{Mn}_2(\text{5-Clsaltn})(\text{H}_2\text{O})_2\text{Fe}(\text{CN})_5(\text{1-CH}_3\text{im})]$  (**3**),  $[\text{Mn}_2(\text{5-Clsaltmen})(\text{H}_2\text{O})_2\text{Fe}(\text{CN})_5(\text{1-CH}_3\text{im})\cdot\text{H}_2\text{O}$  (**4**), and  $[\text{Mn}_2(\text{5-Brsaltmen})_2(\text{H}_2\text{O})_2\text{Fe}(\text{CN})_5(\text{1-CH}_3\text{im})\cdot\text{CH}_3\text{OH}$  (**5**), are neutral and trinuclear with two  $[\text{Mn}(\text{SB})]^+$  ( $\text{SB}^{2-}$  = Schiff base ligands) and one  $[\text{Fe}(\text{1-CH}_3\text{im})(\text{CN})_5]^{2-}$ . Complex  $\{[\text{Et}_4\text{N}][\text{Mn}(\text{acacen})\text{Fe}(\text{CN})_5(\text{1-CH}_3\text{im})]\}_n\cdot 6n\text{H}_2\text{O}$  (**6**) is one-dimensional with alternate  $[\text{Mn}(\text{acacen})]^+$  and  $[\text{Fe}(\text{CN})_5(\text{1-CH}_3\text{im})]^{2-}$  units. The two-dimensional complex  $\{[\text{Mn}_4(\text{saltmen})_4\text{Fe}(\text{CN})_5(\text{1-CH}_3\text{im})]\}_n[\text{ClO}_4]_{2n}\cdot 9n\text{H}_2\text{O}$  (**7**) consists of  $\text{Mn}_4\text{Fe}$  units which are further connected by the phenoxo oxygen atoms. Magnetic studies show the presence of ferromagnetic Mn(III)–Fe(III) coupling in the trinuclear compounds with the magnetic coupling constant ( $J$ ) ranging from 4.5 to 6.0  $\text{cm}^{-1}$ , based on the Hamiltonian  $\hat{H} = -2J\hat{S}_{\text{Fe}}(\hat{S}_{\text{Mn}(1)} + \hat{S}_{\text{Mn}(2)})$ . Antiferromagnetic interaction has been observed in complex **6**, whereas ferromagnetic coupling occurs in complex **7**. Complexes **6** and **7** exhibit long-range magnetic ordering with a  $T_N$  value of 4.0 K for **6** and  $T_C$  of 4.8 K for **7**. Complex **6** shows metamagnetic behavior at 2 K, and complex **7** possesses a hysteresis loop with a coercive field of 500 Oe, typical of a soft ferromagnet.

## Introduction

During the past decades, more and more attention has been paid to the research of cyanide-bridged complexes because of their remarkable magnetic, magneto-optical, and electrochemical properties.<sup>1–30</sup> Several different approaches have been employed to design molecule-based magnets that exhibit

spontaneous magnetization. Many Prussian blue analogues  $\text{M}_x[\text{M}'(\text{CN})_6]_y\cdot n\text{H}_2\text{O}$  have been synthesized by the reaction

\* To whom correspondence should be addressed. E-mail: kouhz@mail.tsinghua.edu.cn. Fax: 86-10-62771748.

- (1) Sato, O.; Lyoda, T.; Fujishima, A.; Hashimoto, K. *Science* **1996**, *272*, 704.
- (2) Mallah, T.; Thiebaut, S.; Verdager, M.; Veillet, P. *Science* **1993**, *262*, 1554.
- (3) (a) Holmes, S. M.; Girolami, G. S. *J. Am. Chem. Soc.* **1999**, *121*, 5593. (b) Hatlevik, O.; Buschmann, W. E.; Manson, J. L. *Adv. Mater.* **1999**, *11*, 914. (c) Bleuzen, A.; Lomenech, C.; Escax, V.; Villain, F.; Varret, F.; Cartier dit Moulin, C.; Verdager, M. *J. Am. Chem. Soc.* **2000**, *122*, 6648.
- (4) Ohba, M.; Maruono, N.; Okawa, H.; Enoki, T.; Lator, J.-M. *J. Am. Chem. Soc.* **1994**, *116*, 11566.
- (5) Ohba, M.; Okawa, H. *Coord. Chem. Rev.* **2000**, *198*, 313.
- (6) Baraldo, L. M.; Forlano, P.; Parise, A. R.; Slep, L. D.; Olabe, J. A. *Coord. Chem. Rev.* **2001**, *219–221*, 881.
- (7) Alcock, N. W.; Samotus, A.; Szklarzewicz, J. *J. Chem. Soc., Dalton Trans.* **1993**, 885.
- (8) El Fallah, M. S.; Rentschler, E.; Caneschi, A.; Sessoli, R.; Gatteschi, D. *Angew. Chem., Int. Ed. Engl.* **1996**, *35*, 1947.

- (9) Yi, X.-Y.; Liu, B.; Jiménez-Aparicio, R.; Urbanos, F. A.; Gao, S.; Xu, W.; Chen, J. S.; Song, Y.; Zheng, L.-M. *Inorg. Chem.* **2005**, *44*, 4309.
- (10) Gheorghe, R.; Andruh, M.; Costes, J.-P.; Donnadieu, B. *Chem. Commun.* **2003**, 2778.
- (11) Kou, H.-Z.; Zhou, B. C.; Si, S.-F.; Wang, R.-J. *Eur. J. Inorg. Chem.* **2004**, 401.
- (12) Marvaud, V.; Decroix, C.; Scuille, A.; Guyard-Duhayon, C.; Vaissermann, J.; Gonnet, F.; Verdager, M. *Chem.—Eur. J.* **2003**, *9*, 1678.
- (13) Van Langenberg, K.; Batten, S. R.; Berry, K. J.; Hockless, D. C. R.; Moubaraki, B.; Murray, K. S. *Inorg. Chem.* **1997**, *36*, 5006.
- (14) Karadas, F.; Schelter, E. J.; Prosvirin, A. V.; Bacsá, J.; Dunbar, K. R. *Chem. Commun.* **2005**, 1414.
- (15) Vostrikova, K. E.; Luneau, D.; Wernsdorfer, W.; Rey, P.; Verdager, M. *J. Am. Chem. Soc.* **2000**, *122*, 718.
- (16) Zhong, Z. J.; Seino, H.; Mizobe, Y.; Hidai, M.; Fujishima, A.; Ohkoshi, S.; Hashimoto, K. *J. Am. Chem. Soc.* **2000**, *122*, 2952.
- (17) Larionova, J.; Gross, M.; Pilkington, M.; Andres, H.; Stoeckli-Evans, H.; Gdel, H. U.; Decurtins, S. *Angew. Chem., Int. Ed.* **2000**, *39*, 1605.
- (18) Parker, R. J.; Spiccia, L.; Berry, K. J.; Fallon, G. D.; Moubaraki, B.; Murray, K. S. *Chem. Commun.* **2001**, 333.
- (19) Colacio, E.; Domínguez-Vera, J. M.; Lloret, F.; Rodríguez, A.; Stoeckli-Evans, H. *Inorg. Chem.* **2003**, *42*, 6962.
- (20) Ohba, M.; Usuki, N.; Fukita, N.; Okawa, H. *Inorg. Chem.* **1998**, *37*, 3349.

of cyanide-containing building blocks  $[M'(CN)_6]^{3-}$  ( $M' = Fe, Cr, Mn$ ) with other paramagnetic metallic complexes  $[M(H_2O)_6]^{m+}$ , and some of them exhibit long-range magnetic ordering at considerably high temperatures.<sup>3</sup>

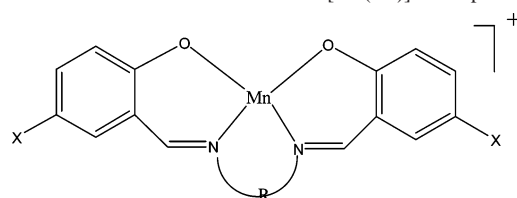
Hybrid Prussian blue complexes were later introduced<sup>44</sup> using the coordinatively unsaturated complexes  $[M(L)]^{m+}$  (where L represents polydentate ligands) instead of  $[M(H_2O)_6]^{m+}$  to react with  $[M'(CN)_6]^{3-}$ . By the alteration of the organic ligands L, a series of polynuclear,<sup>12–18</sup> 1D,<sup>19–21</sup> 2D,<sup>22–24</sup> and 3D<sup>25–28</sup> complexes have been synthesized, which exhibit ferro-, antiferro-, ferri-, or metamagnetic behavior. This approach favors better crystallization and therefore magneto-structural studies, and it affords a rich family of structurally and magnetically different complexes.

Another strategy involving the inclusion of a ligand L to cyanide-containing building blocks,  $[M(L)(CN)_x]^{n-}$  ( $x = 1–5$ ) instead of  $[M'(CN)_6]^{3-}$ , has been developed.<sup>31–44</sup> The presence of L usually lowers the dimensionality of the species and, in the meantime, results in novel molecular structures. It should be noted that some complexes exhibiting SMM

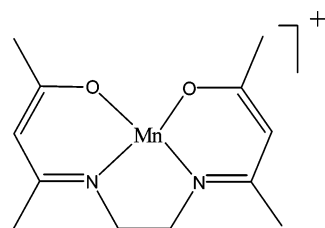
(single-molecule magnet)<sup>38e,39,40,41a</sup> or SCM (single-chain magnet)<sup>41b,42a,42b</sup> behavior have been obtained using this approach.

However, among these  $CN^-$ -containing precursors,  $[M(L)(CN)_5]^{n-}$  (L is a monodentate ligand) has been seldom studied.<sup>44</sup> Interested in the building block  $[Fe(1-CH_3im)(CN)_5]^{2-}$  (1-CH<sub>3</sub>im stands for 1-methylimidazole),<sup>45</sup> we noticed that  $[Fe(1-CH_3im)(CN)_5]^{2-}$  has two interesting characteristics that are different from  $[Fe(CN)_6]^{3-}$ : (i) the electronic configuration  $[3d^5, (3d_{xz})^2(3d_{yz})^2(3d_{xy})^1]$  of the low-spin Fe(III) ion together with the approximate  $C_{4v}$  symmetry of  $[Fe(1-CH_3im)(CN)_5]^{2-}$  and (ii) the divalent form of the anion which should give rise to complexes structurally different from that derived from  $[Fe(CN)_6]^{3-}$ . We used it in our first attempt to perform a reaction with  $[Mn^{III}(SB)]^+$  complexes (SB stands for Schiff base ligands), for the interest of the versatile and flexible structures of  $[Mn(SB)]^+$  complexes that have been widely used to synthesize SMM or SCM complexes.<sup>29,30,46–50</sup> Herein, we report the synthesis,

- (21) El Fallah, M. S.; Ribas, J.; Solans, X.; Font-Bardia, M. *New J. Chem.* **2003**, 27, 895.
- (22) Coronado, E.; Gómez-García, C. J.; Nuez, A.; Romero, F. M.; Rusanov, E.; Stoeckli-Evans, H. *Inorg. Chem.* **2002**, 41, 4615.
- (23) Smith, J. A.; Galán-Mascarós, J.-R.; Clérac, R.; Dunbar, K. R. *Chem. Commun.* **2000**, 1077.
- (24) Thétiot, F.; Triki, S.; Pala, J. S.; Gómez-García, C. J.; Golhen, S. *Chem. Commun.* **2002**, 1078.
- (25) Kou, H.-Z.; Gao, S.; Zhang, J.; Wen, G.-H.; Su, G.; Zheng, R. K.; Zhang, X. X. *J. Am. Chem. Soc.* **2001**, 123, 11809.
- (26) Entley, W. R.; Girolomi, G. S. *Inorg. Chem.* **1994**, 33, 5165.
- (27) Zhang, S. W.; Fu, D. G.; Sun, W. Y.; Hu, Z.; Yu, K. B.; Tang, W. X. *Inorg. Chem.* **2000**, 39, 1142.
- (28) Dong, W.; Zhu, L.-N.; Song, H.-B.; Liao, D.-Z.; Jiang, Z.-H.; Yan, S.-P.; Cheng, P.; Gao, S. *Inorg. Chem.* **2004**, 43, 2465.
- (29) (a) Miyasaka, H.; Matsumoto, N.; Okawa, H.; Re, N.; Gallo, E.; Floriani, C. *Angew. Chem., Int. Ed. Engl.* **1995**, 34, 1446. (b) Miyasaka, H.; Matsumoto, N.; Okawa, H.; Re, N.; Gallo, E.; Floriani, C. *J. Am. Chem. Soc.* **1996**, 118, 981. (c) Miyasaka, H.; Ieda, H.; Matsumoto, N.; Re, N.; Crescenzi, R.; Floriani, C. *Inorg. Chem.* **1998**, 37, 255. (d) Miyasaka, H.; Matsumoto, N.; Re, N.; Gallo, E.; Floriani, C. *Inorg. Chem.* **1997**, 36, 670. (e) Ferbinteanu, M.; Miyasaka, H.; Wernsdorfer, W.; Nakata, K.; Sugiura, K.; Yamashita, M.; Coulon, C.; Clérac, R. *J. Am. Chem. Soc.* **2005**, 127, 3090. (f) Miyasaka, H.; Takahashi, H.; Madanbashi, T.; Sugiura, K.; Clérac, R.; Nojiri, H. *Inorg. Chem.* **2005**, 44, 5969. (g) Miyasaka, H.; Ieda, H.; Matsumoto, N.; Sugiura, K.; Yamashita, M. *Inorg. Chem.* **2003**, 42, 3509. (h) Miyasaka, H.; Okawa, H.; Miyazaki, A.; Enoki, T. *J. Chem. Soc., Dalton Trans.* **1998**, 3991.
- (30) (a) Re, N.; Gallo, E.; Floriani, C.; Miyasaka, H.; Matsumoto, N. *Inorg. Chem.* **1996**, 35, 6004. (b) Miyasaka, H.; Okawa, H.; Miyazaki, A.; Enoki, T. *Inorg. Chem.* **1998**, 37, 4878.
- (31) Abbati, G. L.; Caneschi, A.; Cornia, A.; Fabretti, A. C.; Pozdniakova, Y. A.; Shchegolikina, O. I. *Angew. Chem., Int. Ed.* **2002**, 41, 4517.
- (32) Oshio, H.; Tamada, O.; Onodera, H.; Ito, T.; Ikoma, T.; Tero-Kubota, S. *Inorg. Chem.* **1999**, 38, 5686.
- (33) Hayami, S.; Gu, Z.-Z.; Einaga, Y.; Kobayashi, Y.; Ishikawa, Y.; Yamada, Y.; Fujishima, A.; Sato, O. *Inorg. Chem.* **2001**, 40, 3240.
- (34) (a) Ni, Z.-H.; Kou, H.-Z.; Zhang, L.-F.; Ge, C.; Cui, A.-L.; Wang, R.-J.; Li, Y.; Sato, O. *Angew. Chem., Int. Ed.* **2005**, 44, 7742. (b) Ni, Z.-H.; Kou, H.-Z.; Zhao, Y.-H.; Zheng, L.; Wang, R.-J.; Cui, A.-L.; Sato, O. *Inorg. Chem.* **2005**, 44, 2050.
- (35) Matsumoto, N.; Sunatsuki, Y.; Miyasaka, H.; Hashimoto, Y.; Luneau, D.; Tuchagues, J.-P. *Angew. Chem., Int. Ed.* **1999**, 38, 171.
- (36) (a) Yeung, W.-F.; Man, W.-L.; Wong, W.-T.; Lau, T.-C.; Gao, S. *Angew. Chem., Int. Ed.* **2001**, 40, 3031. (b) Yeung, W.-F.; Lau, P.-H.; Lau, T.-C.; Wei, H.-Y.; Sun, H.-L.; Gao, S.; Chen, Z.-D.; Wong, W.-T. *Inorg. Chem.* **2005**, 44, 6579.
- (37) (a) Lescouëzec, R.; Vaissermann, J.; Lloret, F.; Julve, M.; Verdager, M. *Inorg. Chem.* **2002**, 41, 5943. (b) Lescouëzec, R.; Vaissermann, J.; Toma, L. M.; Carrasco, R.; Lloret, F.; Julve, M. *Inorg. Chem.* **2004**, 43, 2234.
- (38) (a) Yang, J. Y.; Shores, M. P.; Sokol, J. J.; Long, J. R. *Inorg. Chem.* **2003**, 42, 1403. (b) Berseth, P. A.; Sokol, J. J.; Shores, M. P.; Heinrich, J. L.; Long, J. R. *J. Am. Chem. Soc.* **2000**, 122, 9655. (c) Sokol, J. J.; Shores, M. P.; Long, J. R. *Angew. Chem., Int. Ed.* **2001**, 40, 236. (d) Shores, M. P.; Sokol, J. J.; Long, J. R. *J. Am. Chem. Soc.* **2002**, 124, 2279. (e) Sokol, J. J.; Hee, A. G.; Long, J. R. *J. Am. Chem. Soc.* **2002**, 124, 7656.
- (39) Li, D.; Parkin, S.; Wang, G.; Yee, G. T.; Prosvirin, A. V.; Holmes, S. M. *Inorg. Chem.* **2005**, 44, 4903.
- (40) Schelter, E. J.; Prosvirin, A. V.; Dunbar, K. R. *J. Am. Chem. Soc.* **2004**, 126, 15004.
- (41) (a) Wang, S.; Zuo, J.-L.; Zhou, H.-C.; Choi, H. J.; Ke, Y.; Long, J. R.; You, X.-Z. *Angew. Chem., Int. Ed.* **2004**, 43, 5940. (b) Wang, S.; Zuo, J.-L.; Gao, S.; Song, Y.; Zhou, H.-C.; Zhang, Y.-Z.; You, X.-Z. *J. Am. Chem. Soc.* **2004**, 126, 8900.
- (42) (a) Lescouëzec, R.; Vaissermann, J.; Ruiz-Pérez, C.; Lloret, F.; Carrasco, R.; Julve, M.; Verdager, M.; Dromzee, Y.; Gatteschi, D.; Wernsdorfer, W. *Angew. Chem., Int. Ed.* **2003**, 42, 1483. (b) Toma, L. M.; Lescouëzec, R.; Lloret, F.; Julve, M.; Vaissermann, J.; Verdager, M. *Chem. Commun.* **2003**, 1850. (c) Lescouëzec, R.; Lloret, F.; Julve, M.; Vaissermann, J.; Verdager, M.; Llusar, R.; Uriel, S. *Inorg. Chem.* **2001**, 40, 2065. (d) Lescouëzec, R.; Lloret, F.; Julve, M.; Vaissermann, J.; Verdager, M. *Inorg. Chem.* **2002**, 41, 818. (e) Toma, L. M.; Lescouëzec, R.; Toma, L. D.; Lloret, F.; Julve, M.; Vaissermann, J.; Andruh, M. *J. Chem. Soc., Dalton Trans.* **2002**, 3171.
- (43) (a) Zhang, Y.-Z.; Gao, S.; Wang, Z.-M.; Su, G.; Sun, H.-L.; Pan, F. *Inorg. Chem.* **2005**, 44, 4534. (b) Zhang, Y.-Z.; Gao, S.; Sun, H.-L.; Su, G.; Wang, Z.-M.; Zhang, S.-W. *Chem. Commun.* **2004**, 1906.
- (44) Culp, J. T.; Park, J. H.; Meisel, M. W.; Talham, D. R. *Inorg. Chem.* **2003**, 42, 2842.
- (45) (a) Johnson, C. R.; Shepherd, R. E. *Synth. React. Inorg. Met.–Org. Chem.* **1984**, 14, 339. (b) Johnson, C. R.; Shepherd, R. E.; Marr, B.; O'Donnell, S.; Dressick, W. *J. Am. Chem. Soc.* **1980**, 102, 6227. (c) Johnson, C. R.; Shepherd, R. E. *Inorg. Chem.* **1983**, 22, 3506. (d) Johnson, C. R.; Jones, C. M.; Asher, S. A.; Abola, J. E. *Inorg. Chem.* **1991**, 30, 2120.
- (46) (a) Przychodzeń, P.; Lewiński, K.; Bałanda, M.; Pelka, R.; Rams, M.; Wasutyński, T.; Guyard-Duhayon, C.; Sieklucka, B. *Inorg. Chem.* **2004**, 43, 2967. (b) Przychodzeń, P.; Rams, M.; Guyard-Duhayon, C.; Sieklucka, B. *Inorg. Chem. Commun.* **2005**, 8, 350.
- (47) Kou, H.-Z.; Ni, Z.-H.; Zhou, B.-C.; Wang, R.-J. *Inorg. Chem. Commun.* **2004**, 7, 1150.
- (48) (a) Choi, H. J.; Sokol, J. J.; Long, J. R. *J. Phys. Chem. Solids.* **2004**, 65, 839. (b) Shen, X.; Li, B.; Zou, J.; Xu, Z. *Transition Met. Chem.* **2002**, 27, 372. (c) Choi, H. J.; Sokol, J. J.; Long, J. R. *Inorg. Chem.* **2004**, 43, 1606.
- (49) (a) Miyasaka, H.; Nezu, T.; Sugimoto, K.; Sugiura, K.; Yamashita, M.; Clérac, R. *Inorg. Chem.* **2004**, 43, 5486. (b) Miyasaka, H.; Clérac, R.; Mizushima, K.; Sugiura, K.; Yamashita, M.; Wernsdorfer, W.; Coulon, C. *Inorg. Chem.* **2003**, 42, 8203. (c) Miyasaka, H.; Nezu, T.; Sugimoto, K.; Sugiura, K.; Yamashita, M.; Clérac, R. *Chem.–Eur. J.* **2005**, 11, 1592.
- (50) Si, S.-F.; Tang, J.-K.; Liu, Z.-Q.; Liao, D.-Z.; Jiang, Z.-H.; Yan, S.-P.; Cheng, P. *Inorg. Chem. Commun.* **2003**, 6, 1109.

**Scheme 1.** Schematic Illustration of the  $[\text{Mn}(\text{SB})]^+$  Compounds

| SB                        | R   | X  |
|---------------------------|---|----|
| 5-Brsalen <sup>2-</sup>   | CH <sub>2</sub> CH <sub>2</sub>                                   | Br |
| 5-Clsalen <sup>2-</sup>   | CH <sub>2</sub> CH <sub>2</sub>                                   | Cl |
| 5-Clsaltn <sup>2-</sup>   | CH <sub>2</sub> CH <sub>2</sub> CH <sub>2</sub>                   | Cl |
| saltmen <sup>2-</sup>     | C(CH <sub>3</sub> ) <sub>2</sub> C(CH <sub>3</sub> ) <sub>2</sub> | H  |
| 5-Clsaltmen <sup>2-</sup> | C(CH <sub>3</sub> ) <sub>2</sub> C(CH <sub>3</sub> ) <sub>2</sub> | Cl |
| 5-Brsaltmen <sup>2-</sup> | C(CH <sub>3</sub> ) <sub>2</sub> C(CH <sub>3</sub> ) <sub>2</sub> | Br |

SB = acacen<sup>2-</sup>

crystal structures, and magnetic properties of seven complexes derived from  $[\text{Mn}(\text{SB})]^+$  and  $[\text{Fe}(\text{1-CH}_3\text{im})(\text{CN})_5]^{2-}$ . The  $[\text{Mn}(\text{SB})]^+$  complexes employed in the experiments are shown in Scheme 1.

## Experimental Section

Elemental analyses of carbon, hydrogen, and nitrogen were carried out with an Elementary Vario El. The infrared spectroscopy on KBr pellets was performed on a Magna-IR 750 spectrophotometer in the 4000–400  $\text{cm}^{-1}$  region. Magnetic measurements were performed on a Quantum Design MPMS SQUID magnetometer. The experimental susceptibilities were corrected for the diamagnetism of the constituent atoms (Pascal's tables).<sup>51</sup>

**Synthesis.** All chemicals and solvents used for the synthesis were reagent grade. The precursor,  $[\text{Mg}(\text{1-CH}_3\text{im})_2(\text{H}_2\text{O})_2\text{Fe}(\text{CN})_5(\text{1-CH}_3\text{im})\cdot\text{H}_2\text{O}]$ , was prepared according to the literature method.<sup>45d</sup> The Mn(III) Schiff base compounds  $[\text{Mn}(\text{5-Brsalen})(\text{H}_2\text{O})]\text{ClO}_4$ ,  $[\text{Mn}(\text{5-Clsalen})(\text{H}_2\text{O})]\text{ClO}_4$ ,  $[\text{Mn}(\text{5-Clsaltn})(\text{H}_2\text{O})]\text{ClO}_4$ ,  $[\text{Mn}(\text{saltmen})(\text{H}_2\text{O})]\text{ClO}_4$ ,  $[\text{Mn}(\text{5-Brsaltmen})(\text{H}_2\text{O})]\text{ClO}_4$ ,  $[\text{Mn}(\text{5-Clsaltmen})(\text{H}_2\text{O})]\text{ClO}_4$ , and  $[\text{Mn}(\text{acacen})]\text{ClO}_4$  were prepared as described elsewhere.<sup>29,46,47</sup> **Caution:** Perchlorate salts of metal complexes with organic ligands are potentially explosive and should be handled in small quantities with care.

**Complexes 1–5 and 7.** The compounds were similarly prepared as dark brown crystals with the use of appropriate manganese(III) Schiff base complexes; therefore, only the synthesis of complex **1** was described in detail. A methanol solution (10 mL) of  $[\text{Mn}(\text{5-Brsalen})(\text{H}_2\text{O})]\text{ClO}_4$  (0.2 mmol, 101.6 mg) was carefully layered onto an aqueous solution (10 mL) of  $[\text{Mg}(\text{1-CH}_3\text{im})_2(\text{H}_2\text{O})_2\text{Fe}(\text{CN})_5(\text{1-CH}_3\text{im})\cdot\text{H}_2\text{O}]$  (0.1 mmol, 51.1 mg). After the mixture stood for a few weeks in a dark room, dark brown crystals suitable for X-ray diffraction were obtained. They were filtered, washed with 1:1 (v/v) methanol–water, and dried at room temperature. Complex **1**. Yield: 43.2 mg (33.7%). Anal. Calcd. for  $\text{FeMn}_2\text{C}_{41}\text{N}_{11}\text{H}_{36}\text{O}_7\text{Br}_4$ :

C, 38.47; H, 2.83; N, 12.04. Found: C, 38.70; H, 3.06; N, 12.25. IR (KBr):  $\nu$  2137, 2110 ( $\text{C}\equiv\text{N}$ ), 1633  $\text{cm}^{-1}$  ( $\text{C}=\text{N}$ ). Complex **2**. Yield: 47.4 mg (43.0%). Anal. Calcd. for  $\text{FeMn}_2\text{C}_{41}\text{N}_{11}\text{H}_{36}\text{O}_7\text{Cl}_4$ : C, 44.67; H, 3.29; N, 13.98. Found: C, 44.84; H, 3.36; N, 13.99. IR (KBr):  $\nu$  2119 ( $\text{C}\equiv\text{N}$ ), 1631  $\text{cm}^{-1}$  ( $\text{C}=\text{N}$ ). Complex **3**. Yield: 25.6 mg (23%). Anal. Calcd. for  $\text{FeMn}_2\text{C}_{43}\text{N}_{11}\text{H}_{38}\text{O}_6\text{Cl}_4$ : C, 45.69; H, 3.57; N, 13.85. Found: C, 45.83; H, 3.44; N, 13.52. IR (KBr):  $\nu$  2127 ( $\text{C}\equiv\text{N}$ ), 1617  $\text{cm}^{-1}$  ( $\text{C}=\text{N}$ ). Complex **4**. Yield: 45.6 mg (37.5%). Anal. Calcd. for  $\text{FeMn}_2\text{C}_{49}\text{N}_{11}\text{H}_{52}\text{O}_7\text{Cl}_4$ : C, 48.46; H, 4.32; N, 12.69. Found: C, 48.07; H, 4.37; N, 13.11. IR (KBr):  $\nu$  2130, 2117 ( $\text{C}\equiv\text{N}$ ), 1608  $\text{cm}^{-1}$  ( $\text{C}=\text{N}$ ). Complex **5**. Yield: 25 mg (17.8%). Anal. Calcd. for  $\text{FeMn}_2\text{C}_{50}\text{H}_{54}\text{N}_{11}\text{O}_7\text{Br}_4$ : C, 42.80; H, 3.88; N, 10.99. Found: C, 43.01; H, 4.07; N, 10.81. IR (KBr):  $\nu$  2129, 2115 ( $\text{C}\equiv\text{N}$ ), 1613  $\text{cm}^{-1}$  ( $\text{C}=\text{N}$ ). Complex **7**. Yield: 30.4 mg (28.4%). Anal. Calcd. for  $\text{FeMn}_4\text{C}_{89}\text{N}_{15}\text{H}_{112}\text{O}_{25}\text{Cl}_2$ : C, 49.99; H, 5.28; N, 9.82. Found: C, 50.01; H, 5.17; N, 10.18. IR (KBr):  $\nu$  2125 ( $\text{C}\equiv\text{N}$ ), 1602 ( $\text{C}=\text{N}$ ), 1097  $\text{cm}^{-1}$  (Cl–O).

$\{[\text{Et}_4\text{N}][\text{Mn}(\text{acacen})\text{Fe}(\text{CN})_5(\text{1-CH}_3\text{im})]\}_n\cdot n\text{H}_2\text{O}$  (**6**). Complex **6** was synthesized by a similar procedure for the synthesis of  $[\text{Et}_4\text{N}]_2[\text{Mn}(\text{acacen})\text{Fe}(\text{CN})_6]$ .<sup>30a</sup> To an ethanol solution (20 mL) of  $\text{Et}_4\text{NBr}$  (0.2 mmol, 42.0 mg) was added  $[\text{Mg}(\text{1-CH}_3\text{im})_2(\text{H}_2\text{O})_2\text{Fe}(\text{CN})_5(\text{1-CH}_3\text{im})\cdot\text{H}_2\text{O}]$  (0.1 mmol, 51.0 mg). A minimum amount of water (1 mL) was added to this mixture, and it was stirred at room temperature until the solids dissolved completely. The resulting solution was then added dropwise to an ethanol solution (10 mL) of  $[\text{Mn}(\text{acacen})]\text{ClO}_4$  (0.1 mmol, 37.7 mg). After filtration, the filtrate was added to 20 mL of 2-propanol, and then the mixture was allowed to stand in the dark. After a few days, dark brown platelet single crystals suitable for X-ray diffraction formed. They were collected by filtration, washed with 1:1 (v/v) 2-propanol–ethanol, and dried at room temperature. Yield: 23.5 mg (30%). Anal. Calcd. for  $\text{FeMnC}_{29}\text{N}_{10}\text{H}_{56}\text{O}_8$ : C, 44.45; H, 7.20; N, 17.87. Found: C, 44.30; H, 6.96; N, 18.09. IR (KBr):  $\nu$  2115 ( $\text{C}\equiv\text{N}$ ), 1593  $\text{cm}^{-1}$  ( $\text{C}=\text{N}$ ).

**X-ray Structure Determinations.** The data collections of **1** and **2–7** were made on a computer-controlled Siemens P4 diffractometer and a Rigaku R-axis rapid IP equipped with graphite-monochromated Mo  $\text{K}\alpha$  radiation ( $\lambda = 0.71073$  Å), respectively. All the structures were solved by the direct method (SHELXS-97) and refined by full matrix least-squares (SHELXL-97) on  $F^2$ . Anisotropic thermal parameters were used for the non-hydrogen atoms and isotropic parameters for the hydrogen atoms. Hydrogen atoms were added geometrically and refined by using a riding model. In complex **2**, the 1-methylimidazole and its opposite cyano groups around the Fe(III) ion experience disorder. In complex **6**, disorder also exists in the tetraethylammonium cations over two symmetry-related sets of positions. In complex **7**, when the compound crystallized in the space group  $I4/m$ , the presence of a  $C_4$  rotational axis through the Fe(1) [0.500, 0.500, 0.227], C(2) [0.500, 0.500, 0.156], and N(2) [0.500, 0.500, 0.114] atoms results in the disorder of the 1-methylimidazole group opposite to the cyano ligand C(2)–N(2). The interlayer perchlorate ions and water molecules could not be accurately determined. We have tried different single crystals of complex **7** for X-ray diffraction, but the  $R$  factors could not be lowered markedly. Nevertheless, the positions of the intralayer atoms were satisfactorily determined.

## Results and Discussion

**Synthesis and General Characterization.** Because the coordination bonds between  $\text{Mg}^{2+}$  and the cyanides are weak,  $[\text{Mg}(\text{1-CH}_3\text{im})_2(\text{H}_2\text{O})_2\text{Fe}(\text{CN})_5(\text{1-CH}_3\text{im})\cdot\text{H}_2\text{O}]$  is soluble in water to generate free  $[\text{Fe}(\text{CN})_5(\text{1-CH}_3\text{im})]^{2-}$  anions, which

(51) (a) Carlin, R. L. *Magnetochemistry*; Springer-Verlag: Berlin, 1986.  
(b) Kahn, O. *Molecular Magnetism*; Wiley-VCH: New York, 1993.

**Table 1.** Crystallographic Data for Complexes 1–7

|   | 1  | 2  | 3  | 4  |
|---|--|--|--|--|
| formula                                     | FeMn <sub>2</sub> C <sub>41</sub> H <sub>36</sub> N <sub>11</sub> O <sub>7</sub> Br <sub>4</sub> | FeMn <sub>2</sub> C <sub>41</sub> H <sub>36</sub> N <sub>11</sub> O <sub>7</sub> Cl <sub>4</sub> | FeMn <sub>2</sub> C <sub>48</sub> H <sub>36</sub> N <sub>11</sub> O <sub>6</sub> Cl <sub>4</sub> | FeMn <sub>2</sub> C <sub>49</sub> H <sub>32</sub> N <sub>11</sub> O <sub>7</sub> Cl <sub>4</sub> |
| fw  | 1280.18  | 1102.34  | 1112.37  | 1214.55  |
| T (K)                                       | 296  | 123  | 113  | 293  |
| cryst syst                                  | monoclinic   | monoclinic   | orthorhombic   | monoclinic   |
| space group                                 | <i>P2<sub>1</sub>/c</i>  | <i>P2<sub>1</sub>/c</i>  | <i>Pca2<sub>1</sub></i>  | <i>P2<sub>1</sub>/c</i>  |
| <i>a</i> (Å)                                | 13.4412(6)   | 11.265(3)  | 15.011(3)  | 14.892(3)  |
| <i>b</i> (Å)                                | 18.8460(8)   | 13.885(4)  | 28.739(6)  | 14.443(3)  |
| <i>c</i> (Å)                                | 19.6663(8)   | 15.027(4)  | 21.756(4)  | 25.420(5)  |
| $\beta$ (deg)                               | 102.2640(10)   | 92.0390(10)  |  | 93.00(3)   |
| <i>V</i> (Å <sup>3</sup> )                  | 4868.0(4)  | 2349.0(12)   | 9386(3)  | 5460.0(19)   |
| <i>Z</i>                                    | 4  | 2  | 8  | 4  |
| $\rho_{\text{calcd}}$ (g cm <sup>-3</sup> ) | 1.747  | 1.559  | 1.574  | 1.478  |
| <i>F</i> (000)                              | 2524   | 1118   | 4520   | 2492   |
| data/restraints/params                      | 9579/0/604   | 4569/0/332   | 18329/1/1208   | 9271/0/668   |
| R1 [ <i>I</i> > 2 $\sigma$ ( <i>I</i> )]    | 0.0585   | 0.0725   | 0.0653   | 0.0570   |
| wR2 (all data)                              | 0.1362   | 0.1604   | 0.1195   | 0.0926   |

|   | 5  | 6  | 7  |
|---|--|--|--|
| formula                                     | FeMn <sub>2</sub> C <sub>50</sub> H <sub>54</sub> N <sub>11</sub> O <sub>7</sub> Br <sub>4</sub> | FeMnC <sub>29</sub> H <sub>56</sub> N <sub>10</sub> O <sub>8</sub> | FeMn <sub>4</sub> C <sub>89</sub> H <sub>112</sub> N <sub>15</sub> O <sub>25</sub> Cl <sub>2</sub> |
| fw  | 1406.41  | 783.63   | 2138.45  |
| T (K)                                       | 293  | 123  | 173  |
| cryst syst                                  | monoclinic   | orthorhombic   | tetragonal   |
| space group                                 | <i>P2<sub>1</sub>/c</i>  | <i>Pbcm</i>  | <i>I4/m</i>  |
| <i>a</i> (Å)                                | 14.966(7)  | 11.994(3)  | 18.805(3)  |
| <i>b</i> (Å)                                | 14.423(7)  | 18.333(4)  | 18.805(3)  |
| <i>c</i> (Å)                                | 25.709(10)   | 17.220(4)  | 27.473(6)  |
| $\beta$ (deg)                               | 92.97(2)   |  |  |
| <i>V</i> (Å <sup>3</sup> )                  | 5542(4)  | 3786.6(14)   | 9715(3)  |
| <i>Z</i>                                    | 4  | 4  | 4  |
| $\rho_{\text{calcd}}$ (g cm <sup>-3</sup> ) | 1.686  | 1.375  | 1.462  |
| <i>F</i> (000)                              | 2812   | 1660   | 4444   |
| data/restraints/params                      | 19635/0/677  | 3233/0/299   | 4887/0/332   |
| R1 [ <i>I</i> > 2 $\sigma$ ( <i>I</i> )]    | 0.0497   | 0.0735   | 0.1326   |
| wR2 (all data)                              | 0.1344   | 0.1619   | 0.2885   |

makes it possible to prepare new cyanide-bridged magnetic materials. Complexes **1–5** and **7** were all obtained as well-shaped single crystals by the reactions of the appropriate [Mn(SB)(H<sub>2</sub>O)]ClO<sub>4</sub> complexes with [Mg(1-CH<sub>3</sub>im)<sub>2</sub>(H<sub>2</sub>O)<sub>2</sub>·Fe(CN)<sub>5</sub>(1-CH<sub>3</sub>im)]·H<sub>2</sub>O in a molar ratio of 2:1 by the slow diffusion method, while complex **6** was synthesized in the presence of a large countercation [Et<sub>4</sub>N]<sup>+</sup>. Because of the divalent form of the [Fe(CN)<sub>5</sub>(1-CH<sub>3</sub>im)]<sup>2-</sup> building block and the 2:1 molar ratio of Mn:Fe in the final products, the trinuclear products are neutral. The introduction of different [Mn(SB)]<sup>+</sup> compounds results in structurally different products: cis-trinuclear for **1**, trans-trinuclear for **2–5**, 1D chain for **6**, and 2D network for **7**.

Infrared spectra for complexes **1–7** show one or two peaks in the range of 2110–2130 cm<sup>-1</sup>, which are attributable to the C≡N stretching vibration of cyano ligands. The IR spectrum of complex **7** exhibits a strong absorption at 1097 cm<sup>-1</sup>, which can be assigned to the Cl–O stretching vibration for the perchlorate anions. This is consistent with the presence of ClO<sub>4</sub><sup>-</sup> anions from the single-crystal X-ray data.

Detailed crystallographic data for all compounds are listed in Table 1. The labeling schemes for the crystal structures of complexes **1–7** are depicted in Figures 1–5 and in the Supporting Information, and selected bond length and angles are presented in Tables 2–5. The relevant bond distances and angles for **3** and **7** are given as Supporting Information.

**Crystal Structures.** The asymmetric unit of complex **1** consists of one [Fe(CN)<sub>5</sub>(1-CH<sub>3</sub>im)]<sup>2-</sup> anion and two [Mn(5-Brsalen)]<sup>+</sup> cations, as shown in Figure 1. Each [Fe(CN)<sub>5</sub>(1-

CH<sub>3</sub>im)]<sup>2-</sup> unit uses two *cis*-cyano groups to connect with two [Mn(5-Brsalen)]<sup>+</sup> groups, whereas the three remaining CN<sup>-</sup> units are terminal. Two *cis*-bridging cyanides are in the equatorial plane of Fe(III) coordination octahedron. The C–Fe–C bond angles are very close to 90°, while the N(6)–Fe(1)–C(4) group is nearly linear. The Fe–C distances range from 1.924(8)–1.938(7) Å, whereas the Fe–N distance of 1.988(5) Å is a little longer than that of 1.950(2) Å in the precursor [Mg(1-CH<sub>3</sub>im)(H<sub>2</sub>O)<sub>2</sub>Fe(CN)<sub>5</sub>(1-CH<sub>3</sub>im)]·H<sub>2</sub>O.<sup>45d</sup>

The coordination geometry of the Mn(III) ion in complex **1** is elongated octahedral because of the Jahn–Teller Effect of the high-spin d<sup>4</sup> electronic configuration of Mn(III). The equatorial sites are occupied by the N<sub>2</sub>O<sub>2</sub> donor atoms of the 5-Brsalen<sup>2-</sup> ligand with average bond distances of Mn–N = 1.976(5) Å and Mn–O = 1.880(4) Å, while the two axial positions are occupied by the N atom of the cyanide group of [Fe(CN)<sub>5</sub>(1-CH<sub>3</sub>im)]<sup>2-</sup> and a water molecule with the Mn–O distances of 2.289(4) Å for Mn(1)–O(1W) and 2.266(4) Å for Mn(1)–O(2W). The Mn(1)–N(1) and Mn(2)–N(2) bond distances are 2.236(6) and 2.222(6) Å, respectively, and the Mn–N≡C bond angles are bent [Mn(1)–N(1)–C(1) = 160.0(5)° and Mn(2)–N(4)–C(4) = 154.3(5)°]. The adjacent Fe–Mn distances are 5.250(5) Å for Fe(1)–Mn(1) and 5.119(5) Å for Fe(1)–Mn(2). The bond distances and angles are similar to those found in the [Mn(SB)]<sub>m</sub>[Fe(CN)<sub>6</sub>]<sub>n</sub> complexes.<sup>29c,29d</sup>

Figure 1b shows the cell packing diagram of complex **1** along the *a* axis. There are hydrogen-bond interactions among the cyano nitrogen atoms (N(3) and N(5)) of the trinuclear

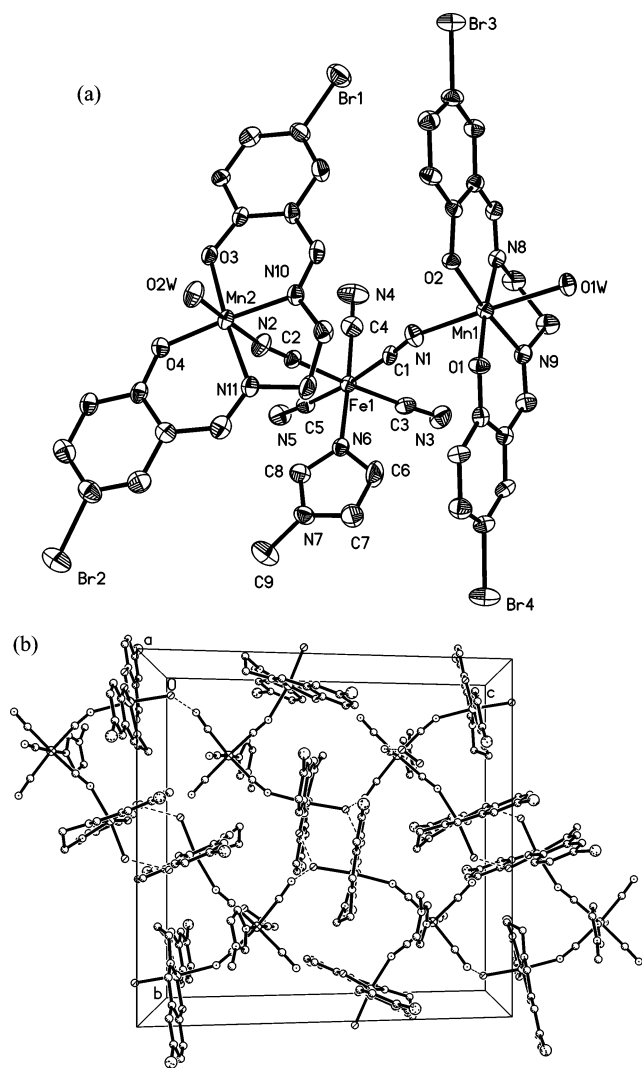


**Figure 1.** (a) cis-Trinuclear structure of complex **1** with atom-labeling scheme showing 30% probability thermal ellipsoids (hydrogen atoms and crystallized water molecules are omitted for clarity). (b) The cell packing of **1** along the *a* axis.

**Table 2.** Selected Bond Distances (Å) and Angles (deg) of Complex **1**

|                 |          |                 |          |
|-----------------|----------|-----------------|----------|
| Fe(1)–C(1)      | 1.936(7) | Fe(1)–C(2)      | 1.933(7) |
| Fe(1)–C(3)      | 1.935(8) | Fe(1)–C(4)      | 1.924(8) |
| Fe(1)–C(5)      | 1.938(7) | Fe(1)–N(6)      | 1.988(5) |
| C(1)–N(1)       | 1.145(7) | C(2)–N(2)       | 1.139(7) |
| C(3)–N(3)       | 1.160(8) | C(4)–N(4)       | 1.155(9) |
| C(5)–N(5)       | 1.140(7) | C(9)–N(7)       | 1.449(9) |
| Mn(1)–N(1)      | 2.236(6) | Mn(1)–O(1W)     | 2.289(4) |
| Mn(1)–O(1)      | 1.866(4) | Mn(1)–N(8)      | 1.977(5) |
| Mn(1)–O(2)      | 1.888(4) | Mn(1)–N(9)      | 1.981(5) |
| Mn(2)–N(2)      | 2.222(6) | Mn(2)–O(2W)     | 2.266(4) |
| Mn(2)–O(3)      | 1.880(4) | Mn(2)–N(10)     | 1.969(5) |
| Mn(2)–O(4)      | 1.887(4) | Mn(2)–N(11)     | 1.979(5) |
| Mn(1)–N(1)–C(1) | 160.0(5) | N(1)–C(1)–Fe(1) | 176.7(6) |
| Mn(2)–N(2)–C(2) | 154.3(5) | N(2)–C(2)–Fe(1) | 173.5(6) |

entities and the oxygen atoms of 5-Brsalen ligands (O(2) and O(4)), coordinated water molecules, and solvent water molecules. Each coordinated water molecule is involved in two H-bonding interactions with D–A separations ranging from 2.843 to 2.976 Å. As shown in Figure 1b, each trinuclear unit is surrounded by six symmetry-related trinuclear units through hydrogen bonds. These abundant hydrogen-bond interactions form a 2D network.

**Table 3.** Selected Bond Distances (Å) and Angles (deg) of Complex **2**

|                 |          |                 |          |
|-----------------|----------|-----------------|----------|
| Fe(1)–C(1)      | 1.918(6) | Fe(1)–C(2)      | 1.939(5) |
| Fe(1)–C(3)      | 1.86(3)  | Fe(1)–N(4)      | 2.039(7) |
| Mn(1)–N(1)      | 2.243(5) | Mn(1)–O(1W)     | 2.231(3) |
| Mn(1)–O(1)      | 1.879(4) | Mn(1)–O(2)      | 1.883(4) |
| Mn(1)–N(6)      | 1.994(5) | Mn(1)–N(7)      | 1.993(5) |
| Mn(1)–N(1)–C(1) | 149.8(5) | N(1)–C(1)–Fe(1) | 177.9(5) |
| N(2)–C(2)–Fe(1) | 179.7(6) | N(3)–C(3)–Fe(1) | 167(3)   |

**Table 4.** Selected Bond Distances (Å) and Angles (deg) of Complexes **4** and **5**

|                 | <b>4</b> | <b>5</b> |
|-----------------|----------|----------|
| Fe(1)–C(1)      | 1.941(3) | 1.948(3) |
| Fe(1)–C(2)      | 1.928(3) | 1.935(3) |
| Fe(1)–C(3)      | 1.917(4) | 1.926(3) |
| Fe(1)–C(4)      | 1.950(4) | 1.942(3) |
| Fe(1)–C(5)      | 1.941(4) | 1.943(3) |
| Fe(1)–N(6)      | 2.008(3) | 2.009(3) |
| Mn(1)–N(1)      | 2.311(3) | 2.323(3) |
| Mn(2)–N(2)      | 2.258(3) | 2.266(3) |
| Mn(1)–O(1W)     | 2.323(3) | 2.333(2) |
| Mn(1)–O(1)      | 1.878(3) | 1.885(2) |
| Mn(1)–O(2)      | 1.858(3) | 1.882(2) |
| Mn(1)–N(8)      | 1.987(3) | 1.991(2) |
| Mn(1)–N(9)      | 2.000(3) | 1.986(2) |
| Mn(2)–O(3)      | 1.894(3) | 1.893(2) |
| Mn(2)–O(4)      | 1.862(3) | 1.876(2) |
| Mn(2)–N(10)     | 1.984(3) | 1.981(3) |
| Mn(2)–N(11)     | 1.984(3) | 1.986(3) |
| Mn(2)–O(2W)     | 2.422(2) | 2.429(3) |
| Mn(1)–N(1)–C(1) | 159.7(3) | 159.4(2) |
| Mn(2)–N(2)–C(2) | 157.8(3) | 157.2(3) |
| N(1)–C(1)–Fe(1) | 176.5(3) | 177.4(3) |
| N(2)–C(2)–Fe(1) | 175.1(3) | 175.0(3) |

**Table 5.** Selected Bond Distances (Å) and Angles (deg) of Complex **6**

|                 |          |                 |          |
|-----------------|----------|-----------------|----------|
| Fe(1)–C(7)      | 1.949(5) | Fe(1)–C(8)      | 1.943(8) |
| Fe(1)–C(9)      | 1.946(5) | Fe(1)–N(5)      | 1.979(6) |
| Mn(1)–N(1)      | 1.979(4) | Mn(1)–N(2)      | 2.331(4) |
| Mn(1)–O(1)      | 1.902(3) |                 |          |
| Fe(1)–C(7)–N(2) | 177.7(4) | C(7)–N(2)–Mn(1) | 144.4(4) |

Complexes **2–5** are all trans-trinuclear and are similar to each other. In complex **2**, the 1-methylimidazole and its opposite CN<sup>−</sup> groups are disordered (see Figure 2); for complex **3**, each unit cell consists of two independent trans-trinuclear units, one of which is shown in Figure S1. Figure 3 shows the structure of complex **4** to which the structures of complexes **3–5** are similar.

In all the trans-trinuclear compounds, **2–5**, the [Fe(CN)<sub>5</sub>-(1-CH<sub>3</sub>im)]<sup>2−</sup> unit uses two *trans*-CN<sup>−</sup> groups in the equatorial plane to connect two [Mn(SB)]<sup>+</sup> groups. The axial CN<sup>−</sup> group opposite to the 1-methylimidazole ligand is monodentate. All Fe–C distances range from 1.917(4) to 1.969(6) Å (excluding the disordered CN<sup>−</sup> in complex **2**, Fe(1)–C(3) = 1.86(3) Å), and all the Fe–C≡N linkages are always linear. The Fe–N<sub>imidazole</sub> distances in all complexes have similar values, ranging from 1.990(5) to 2.039(7) Å. The Mn(III) ions are coordinated equatorially by N<sub>2</sub>O<sub>2</sub> donors of the tetradentate Schiff base ligands and axially by a cyano nitrogen atom of [Fe(CN)<sub>5</sub>(1-CH<sub>3</sub>im)]<sup>2−</sup> with Mn–N<sub>cyano</sub> bond distances ranging from 2.221(5) to 2.323(3) Å and a water oxygen atom (Mn–O<sub>water</sub> bond distance range of 2.222(4)–2.429(3) Å), giving rise to an elongated octahedral coordination geometry. The bridging cyano ligands coordi-

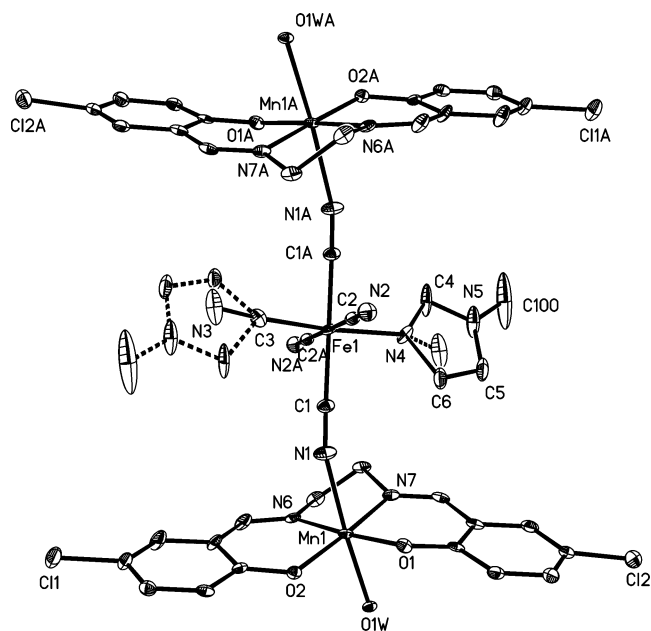


**Figure 2.** Structure of complex **2** with atom-labeling scheme showing 30% probability thermal ellipsoids (hydrogen atoms and crystallized water molecules are omitted for clarity). Dashed lines represent disordered cyano and 1-methylimidazole groups.

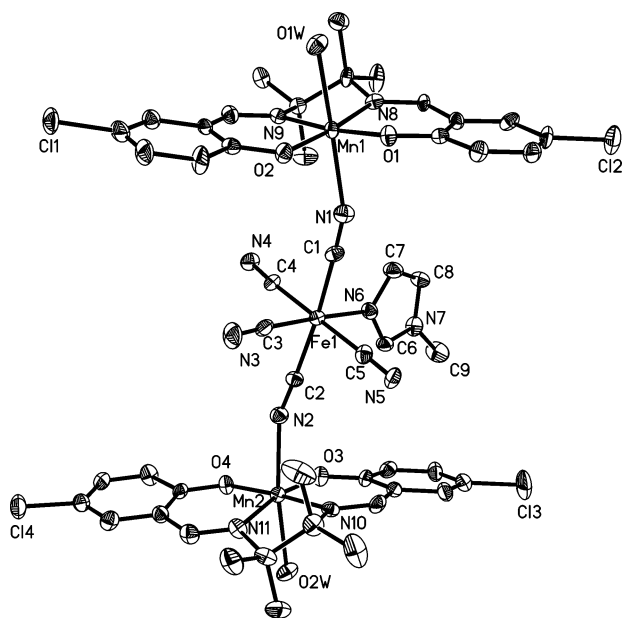


**Figure 3.** Trinuclear structure of complex **4** with atom-labeling scheme showing 30% probability thermal ellipsoids (hydrogen atoms and crystallized water molecules are omitted for clarity). Complex **5** is isostructural to **4** (Cl is replaced by Br).

nate to the Mn(III) ions in a bent fashion with the Mn–N≡C angles ranging from 149.8(5) to 165.2(6)°. The intramolecular Fe–Mn distances are 5.130 Å for **2**, 5.264, 5.189, 5.150, and 5.158 Å for **3**, 5.307 and 5.244 Å for **4**, and 5.325 and 5.249 Å for **5**.

The coordinated water molecules are involved in hydrogen-bonding interactions with the nonbridging cyano nitrogen atoms and the phenoxo atoms of six neighboring trinuclear units, forming 2D networks as in complex **1**.

**Crystal Structure of Complex 6.** As shown in Figure 4, complex **6**,  $\{[Et_4N][Mn(acacen)Fe(CN)_5(1-CH_3im)]\}_n \cdot 6nH_2O$ ,

exhibits a one-dimensional zigzag chain running along the *c* axis with  $(-Fe-C\equiv N-Mn-N\equiv C-)_n$  as the repeating unit. Unlike the 1D analogue,  $[Et_4N]_2[Mn(acacen)Fe(CN)_6]$ , in which  $[Fe(CN)_6]^{3-}$  uses two *trans*-cyano ligands to connect two  $[Mn(acacen)]^+$  units,<sup>30a</sup> the  $[Fe(CN)_5(1-CH_3im)]^{2-}$  units use two *cis*-cyano groups in the equatorial plane to connect with two  $[Mn(acacen)]^+$  moieties. The Fe–C distances varies from 1.943(8) to 1.949(5) Å, while the Fe–N<sub>imidazole</sub> bond distance is 1.979(6) Å. The coordination geometry of the Mn(III) ion is also an elongated octahedron, where the equatorial plane is occupied by N<sub>2</sub>O<sub>2</sub> donor atoms of the *acacen*<sup>2-</sup> ligand with a Mn(1)–N(1) distance of 1.979(4) Å and a Mn(1)–O(1) distance of 1.902(3) Å, and the two axial positions are occupied by the nitrogen atom N(2) from  $[Fe(CN)_5(1-CH_3im)]^{2-}$  [Mn(1)–N(2) = 2.331(4) Å, N(2)–Mn(1)–N(2B) = 172.8(2)°, B indicates a symmetry operation of  $x, 0.5 - y, -z$ ].

The bridging cyanide ligands are coordinated to the Mn(III) ion in a bent fashion with an Mn(1)–N(2)–C(7) bond angle of 144.4(4)°, smaller than that (152.6(3)°) in  $[Et_4N]_2[Mn(acacen)Fe(CN)_6]$ .<sup>30a</sup> The adjacent Fe–Mn distance in the chain is 5.152(5) Å. The disordered  $Et_4N^+$  cations are located among the Fe(III)–Mn(III) chains and act as charge-balancing cations. In addition, solvent water molecules are also positioned among the chains.

**Crystal Structure of Complex 7.** In complex **7**, the four equatorial CN<sup>−</sup> ligands around the Fe(III) ions coordinate axially to the Mn(III) ions from Mn(saltmen) moieties, while the disordered 1-methylimidazole unit and its opposite CN<sup>−</sup> group remains terminal (Supporting Information). As shown in Scheme 2, every two adjacent Mn(saltmen) units are further linked through the Mn–O bonds, which can be widely observed among the  $[Mn^{III}(\text{saltmen})]^+$  Schiff base derivatives.<sup>29b,29e,49</sup> Thus, the  $[-NC-Fe-CN-Mn-O_2-Mn-]$  repeating units lead the complex to a two-dimensional layered structure (Figure 5), with the perchlorate ions and some crystallized water molecules positioned between the layers.

In complex **7**, the Fe(III) ions exhibit a distorted octahedral geometry, with Fe–C bond distances of 1.935(14) and 1.936(8) Å and an Fe–N<sub>imidazole</sub> bond distance of 1.961(13) Å. The coordination geometry of the Mn(III) ions is elongated octahedral with axial coordination bond distances of Mn(1)–N(1) = 2.197(8) Å and Mn(1)–O(1C) = 2.844(8) Å (C indicates the symmetry operation of  $0.5 - x, 0.5 - y, 0.5 - z$ ). The Mn(1)–N(1)–C(1) bond angle of 157.3(7)° shows significant deviation from linearity. The adjacent metal–metal distances are 5.164(8) Å for Fe–Mn and 3.651(8) Å for Mn–Mn.

Another feature of  $[Fe(1-CH_3im)(CN)_5]^{2-}$  lies in the rotation of the imidazole ligand attached to the Fe(III) ion, which is relevant to the electron configuration of Fe(III). The dihedral angle,  $\phi$ , between the imidazole plane and the plane defined by three meridian CN<sup>−</sup> ligands, as shown in Scheme 3, can estimate the situation.<sup>45d</sup> For the present seven complexes and the structurally available complex  $[Mg(1-CH_3im)(H_2O)_2Fe(CN)_5(1-CH_3im)] \cdot H_2O$ ,<sup>45d</sup> the  $\phi$  value ranges from 11.6° for complex **3** to 44.3° for complex **6** (Table 6).

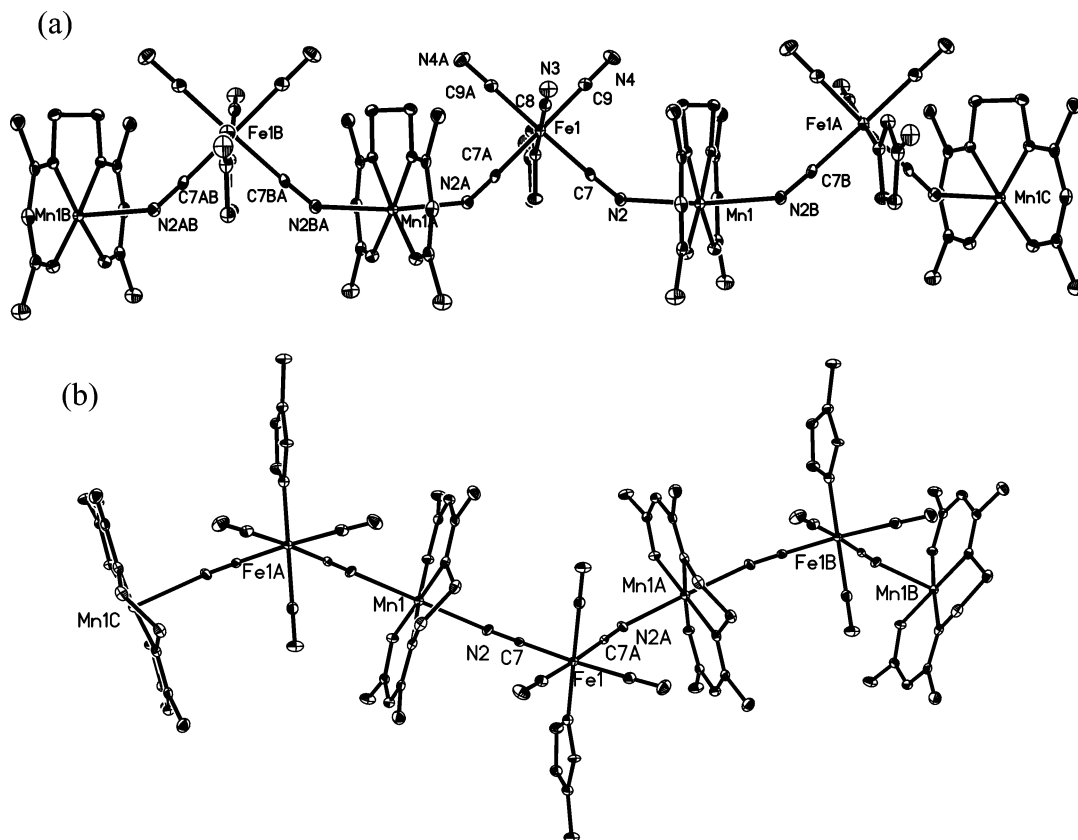
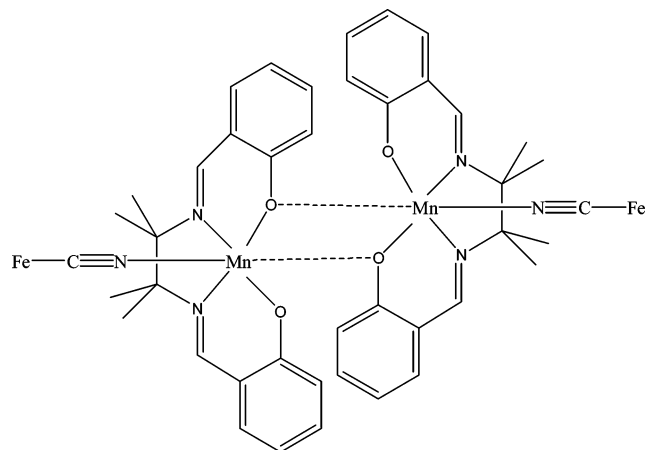


**Figure 4.** One-dimensional chain propagating along the *c* axis in complex 6 with atom-labeling scheme showing 30% probability thermal ellipsoids (hydrogen atoms, disordered tetraethylammonium cations, and crystallized water molecules are omitted for clarity): (a) 1D zigzag chain showing the bent cyanide bridges and (b) view of the chain emphasizing the orientation of the 1-methylimidazole groups.

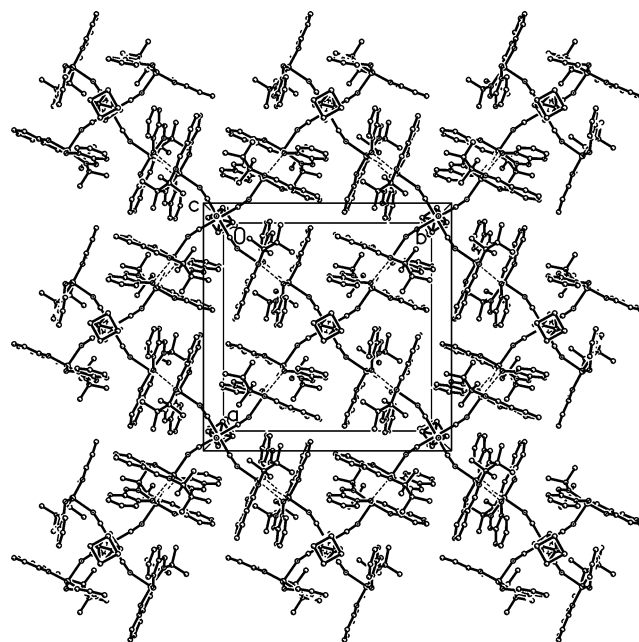
#### Scheme 2



The expectation that the Fe–N(imidazole) bond length is always longer for the smaller  $\phi$  values is basically valid for the present seven complexes.<sup>45d</sup>

**Magnetic Properties of Complexes 1–5.** The magnetic susceptibility was measured from 5 to 300 K, as shown in Figure 6. The magnetic behaviors of complexes 1–5 are quite similar. The room temperature  $\chi_m T$  values are consistent with the presence of high-spin Mn(III) and low-spin Fe(III) ions in 1–5. Table 7 shows the DC magnetic data for the five trinuclear complexes.

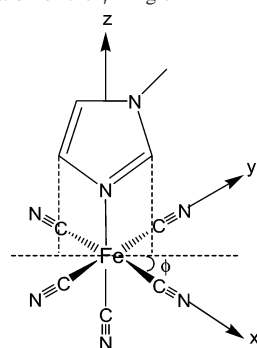
Complexes 1–5 exhibit typical Mn(III)–Fe(III) ferromagnetic interaction with the low-temperature decrease of  $\chi_m T$  attributed to intermolecular antiferromagnetic interaction



**Figure 5.** Layered structure of 7 along the *c* axis (hydrogen atoms, perchlorate ions, and water molecules are omitted for clarity).

and the zero-field splitting term of the Mn(III) ion.<sup>29,30,34a,48c,49,50</sup> At low temperatures, both effects result in similar magnetic behavior.

On the basis of the trimeric model, the magnetic susceptibility data for complexes 1–5 can be fitted by the expressions derived from the isotropic exchange spin Hamil-

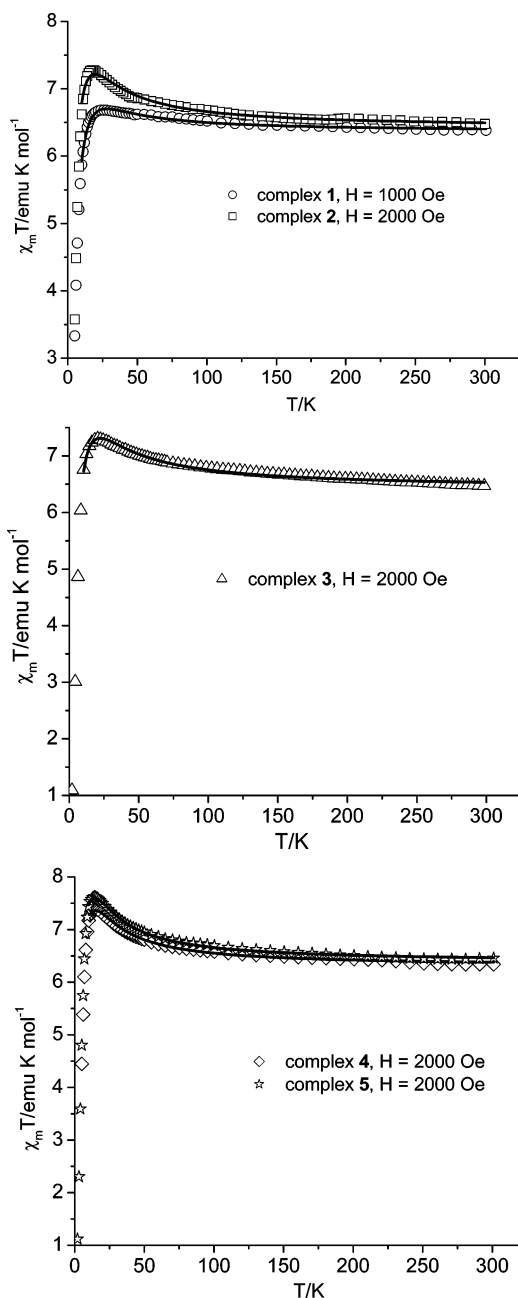
**Scheme 3.** Illustration of the  $\phi$  Angle**Table 6.** Comparison of the Bond Distances for the  $[\text{Fe}(\text{1-CH}_3\text{im})(\text{CN})_5]^{2-}$ -Containing Complexes

| structure | Fe–N(1–CH <sub>3</sub> im) (Å) | $\phi$ (deg) | ref  |           |
|-----------|--------------------------------|--------------|------|-----------|
| <b>1</b>  | trinuclear                     | 1.988(5)     | 37.1 | this work |
| <b>2</b>  | trinuclear                     | 2.039(7)     | 23.0 | this work |
| <b>3</b>  | trinuclear                     | 2.010(6)     | 11.6 | this work |
|           |                                | 1.990(5)     | 33.7 |           |
| <b>4</b>  | trinuclear                     | 2.008(3)     | 15.9 | this work |
| <b>5</b>  | trinuclear                     | 2.009(3)     | 17.0 | this work |
| <b>6</b>  | 1D                             | 1.979(6)     | 44.3 | this work |
| MgFe      | 1D                             | 1.950(2)     | 34.5 | 45d       |
| <b>7</b>  | 2D                             | 1.96(1)      | 42.0 | this work |

tonian  $\hat{H} = -2J\hat{S}_{\text{Fe}}(\hat{S}_{\text{Mn}(1)} + \hat{S}_{\text{Mn}(2)})$ , in which we assume equivalent interactions among the central Fe(III) ion and the two Mn(III) ions and neglect the magnetic interaction between the terminal Mn(III) ions (eq 1 in Supporting Information).

If a molecular field term is taken into account, the final magnetic susceptibility can be obtained over the temperature range of 10–300 K. The obtained best-fit parameters are shown in Table 8. If all data down to 5 K were used for the fitting, no satisfactory results could be obtained, which may be caused by the neglect of the zfs (zero-field splitting) effect of Mn(III) during the fitting. The  $J$  values are on the order of several  $\text{cm}^{-1}$ , close to that for the  $\text{Mn(III)–Fe(III)(CN)}_6$  polynuclear species.<sup>29,48c,49,50</sup>

To include the zfs effect of the ground state ( $S_T = 9/2$  for ferromagnetically coupled  $\text{Mn}_2\text{Fe}$  species **1–5**), eq 3 can be derived from the spin Hamiltonian  $\hat{H} = -2J\hat{S}_{\text{Fe}}(\hat{S}_{\text{Mn}(1)} + \hat{S}_{\text{Mn}(2)}) + D[\hat{S}_z^2 - S(S+1)/3]\delta_{S=9/2}$  (see Supporting Information). It is worth mentioning that this fitting method should be used under the condition that  $J \gg |D|$  and the microstates do not couple with the excited spin states (e.g.,  $S_T = 7/2$ ; Figure 7, the energy diagram for the trinuclear compounds).<sup>51</sup> Once again, the data in the temperature range of 10–300 K were used for the fitting with the best-fit parameters shown in Table 8. The results show that the  $J$  values are slightly larger than that obtained from the former method, and the  $D$  values are approximately double the corresponding  $zJ'$  values. Figure 6 displays the theoretical curves based on the parameters derived from the latter method. Although the powder magnetic susceptibility data could not unambiguously distinguish the negative or positive sign of  $D$ , positive  $D$  values could not give satisfactory fitting results for each trinuclear compound. It suggests the presence of negative zfs parameters for complexes **1–5**.

**Figure 6.** Temperature dependence of  $\chi_m T / \text{Mn}_2\text{Fe}$  for complexes **1–5**. The solid line represents the calculated values using eq 3.**Table 7.** Magnetic Data for the Trinuclear Complexes **1–5**

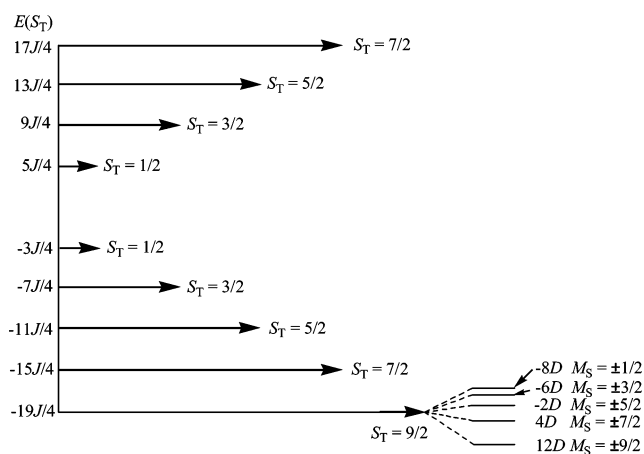
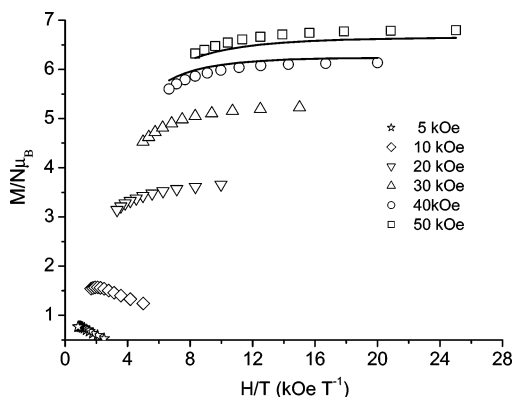
|          | room temp $\chi_m T$<br>(emu K mol <sup>-1</sup> ) | Curie constant<br>(emu K mol <sup>-1</sup> ) | Weiss constant, $\theta$<br>(K) |
|----------|--|--|---------------------------------|
| <b>1</b> | 6.38   | 6.38   | 1.24                            |
| <b>2</b> | 6.49   | 6.49   | 2.51                            |
| <b>3</b> | 6.35   | 6.03   | 3.56                            |
| <b>4</b> | 6.34   | 6.30   | 3.23                            |
| <b>5</b> | 6.46   | 6.38   | 3.51                            |

The magnetization curves below 5 K for complexes **1–5** are very similar, showing a slow increase in magnetization at low magnetic fields (<15 kOe) followed by a sharp increase (Supporting Information). This metamagnetic-like behavior reveals that marked intermolecular antiferromagnetic coupling is present in these complexes. Detailed magnetization measurements at 2–6 K and in the applied

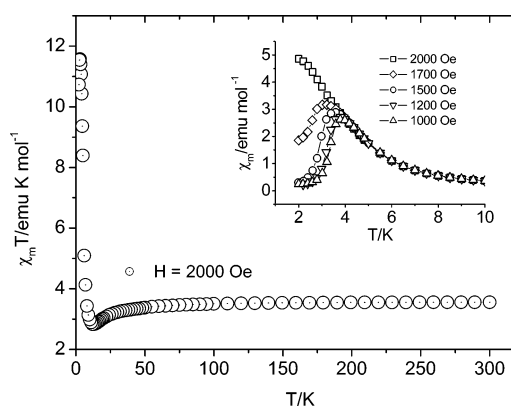
**Table 8.** Comparison of Magnetic Coupling Constants<sup>a</sup>

|          | $\phi$       | Mn–N <sub>cyanano</sub> (Å)               | C≡N–Mn (deg)                              | $J$ (cm <sup>-1</sup> ) | $g$     | $zJ'$ (cm <sup>-1</sup> ) | $D$ (cm <sup>-1</sup> ) |
|----------|--------------|---|---|-------------------------|---------|---------------------------|-------------------------|
| <b>1</b> | 37.1         | 2.236(6), 2.222(6)                        | 160.0(5), 154.3(5)                        | 4.75(6)                 | 2.00(1) | -0.36(1)                  | 0 <sup>b</sup>          |
|          |              |   |   | 5.92(7)                 | 2.04(1) | 0 <sup>b</sup>            | -0.88(1)                |
| <b>2</b> | 23.0         | 2.243(5)                                  | 149.8(5)                                  | 4.98(10)                | 2.01(1) | -0.26(1)                  | 0 <sup>b</sup>          |
|          |              |   |   | 5.86(11)                | 2.04(1) | 0 <sup>b</sup>            | -0.60(1)                |
| <b>3</b> | 11.6<br>33.7 | 2.221(5), 2.249(5);<br>2.229(5), 2.298(5) | 165.2(5), 156.9(5);<br>152.8(5), 147.8(5) | 6.01(8)                 | 2.01(1) | -0.29(1)                  | 0 <sup>b</sup>          |
|          |              |   |   | 6.68(8)                 | 2.01(1) | 0 <sup>b</sup>            | -0.67(1)                |
| <b>4</b> | 15.9         | 2.311(3), 2.258(3)                        | 159.7(3), 157.8(3)                        | 4.51(6)                 | 1.99(1) | -0.19(1)                  | 0 <sup>b</sup>          |
|          |              |   |   | 4.95(6)                 | 1.98(1) | 0 <sup>b</sup>            | -0.43(1)                |
| <b>5</b> | 17.0         | 2.323(3), 2.266(3)                        | 159.4(2), 157.2(3)                        | 4.68(5)                 | 2.00(1) | -0.18(1)                  | 0 <sup>b</sup>          |
|          |              |   |   | 5.10(6)                 | 2.00(1) | 0 <sup>b</sup>            | -0.40(1)                |
| <b>7</b> | 42.0         | 2.197(8)                                  | 157.3(7)                                  | 2.34(7)                 | 2.04(2) | 0.036(4)                  | 0 <sup>b</sup>          |

<sup>a</sup> Greater than 10 K data have been used for the fitting. <sup>b</sup> The value has been set at zero during the fitting process.

**Figure 7.** Energy levels in the  $|S_T, M_S\rangle$  basis diagram for complexes **1–5** (only the zfs effect is considered for the ground state).**Figure 8.** Magnetization vs  $H/T$  plot for complex **5** in the range of 2–6 K and 5–50 kOe. The solid lines represent the best fitting results using the Anisofit 2.0 software.

magnetic field of 10–50 kOe for complex **5** show that the isofield lines are not *superimposable*, indicating the presence of appreciable zfs. Significantly, the 5 and 10 kOe magnetization curves show decrease with the increase of  $H/T$ , suggesting the presence of an obvious intermolecular antiferromagnetic interaction in **5**. The 40 and 50 kOe data were used to fit using the Anisofit 2.0 program<sup>38d</sup> giving parameters of  $g = 1.74$  and  $D = -0.70$  cm<sup>-1</sup> (Figure 8), assuming an  $S = 9/2$  ground state and avoiding the intermolecular magnetic coupling effect. Thus, the spin-reversal energy barrier,  $\Delta E$ , between the  $M_S = 9/2$  and  $-9/2$  spin states can be calculated to be  $\Delta E = 14$  cm<sup>-1</sup> via  $\Delta E = (S^2 - 1/4)|D|$ .

**Figure 9.** Temperature dependence of  $\chi_m T / \text{MnFe}$  for complex **6**. The inset shows field-cooled magnetization for **6** in different applied magnetic fields.

The temperature dependence of the AC magnetic susceptibility at zero DC and 3 Oe AC magnetic field for complex **5** shows that the out-of-phase AC magnetic susceptibility has nonzero values below 4.0 K and is frequency dependent (Supporting Information). This suggests the presence of slow relaxation of magnetization in complex **5**,<sup>52</sup> consistent with the DC magnetic measurements. However, the signals are considerably weak because of the presence of intermolecular magnetic interaction, precluding any quantitative analysis. It is worth mentioning that two Mn<sub>2</sub>Fe complexes based on  $[\text{Fe}(\text{CN})_6]^{3-}$  have been proven to be SMMs.<sup>29e,48c</sup>

The above results suggest that trinuclear compounds **1–5** exhibit ferromagnetic Mn(III)–Fe(III) coupling, in which an axial zfs effect and appreciable intermolecular antiferromagnetic interaction operate, dominating the low-temperature magnetic behavior.

**Magnetic Properties of Complex 6.** The magnetic susceptibility was measured from 2 to 300 K under an applied magnetic field of 2000 Oe. A plot of  $\chi_m T$  versus  $T$  is shown in Figure 9, where  $\chi_m$  is the magnetic susceptibility per MnFe unit. The  $\chi_m T$  value at room temperature is 3.55 emu K mol<sup>-1</sup>. The  $1/\chi_m$  value above 20 K obeys the Curie–Weiss law with a Curie constant of  $C = 3.60$  emu K mol<sup>-1</sup> and a negative Weiss constant of  $\theta = -3.23$  K, indicating an antiferromagnetic interaction between the high-spin Mn(III) ions and the low-spin Fe(III) ions through bridging cyanide

(52) Ge, C.-H.; Cui, A.-L.; Ni, Z.-H.; Jiang, Y.-B.; Zhang, L.-F.; Ribas, J.; Kou, H.-Z. *Inorg. Chem.* **2006**, *45*, 4883.

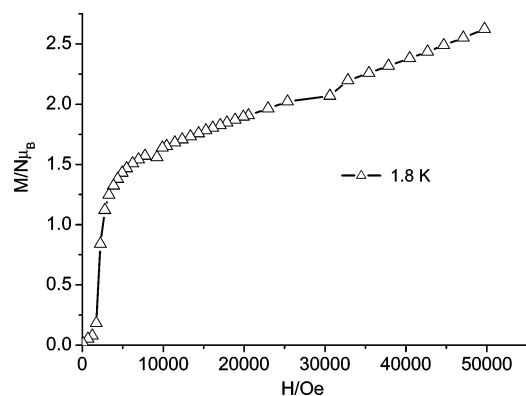


**Figure 10.** Field dependence of magnetization for complex 6. The solid line is a guide for the eye.

groups. When the temperature is lowered,  $\chi_m T$  decreases gradually to reach a minimum of  $2.83 \text{ emu K mol}^{-1}$  at 12.0 K, then increases abruptly to reach a maximum of  $11.57 \text{ emu K mol}^{-1}$  at 3.0 K, and finally decreases again to  $10.73 \text{ emu K mol}^{-1}$  at 2.2 K. The presence of the abrupt increase of  $\chi_m T$  suggests the onset of magnetic ordering.

To confirm the magnetic phase transition at low temperature, we measured the FCM (field-cooled magnetization) curve under different magnetic fields in the temperature range of 2–10 K, and the results are shown in the inset of Figure 9. Below 1700 Oe, the FCM curves show a peak at  $\sim 4 \text{ K}$ , which can be considered as the antiferromagnetic phase transition temperature ( $T_N$ ). This peak disappears when the curve was measured at 2000 Oe, suggesting a typical metamagnetic behavior of this antiferromagnet and the range of 1700–2000 Oe of the critical field ( $H_c$ ).

The metamagnetic behavior was further characterized by the measurements of field-dependent magnetization at 1.8 K. Figure 10 shows that the curve has the sigmoidal shape expected for a metamagnet: the magnetization first increases slowly with the external field because of antiferromagnetic interchain interactions and then increases sharply, showing a phase transition to a ferrimagnetic state. The critical field at 2 K is about 1700 Oe, corresponding to the FCM results. When the field is increased further, the magnetization reaches  $2.4 N\beta$  at the highest measured field (50 kOe) and continues to increase, indicating that saturation (expected value of  $3 N\beta$  for  $S_T = S_{\text{Mn}} - S_{\text{Fe}} = 3/2$ ) has not yet been achieved. Such behavior can be often observed in  $[\text{Mn}(\text{SB})]^+$ -containing compounds<sup>29</sup> because of the large zero-field splitting of the Mn(III) ions.

**Magnetic Properties of Complex 7.** The magnetic susceptibility was measured from 2 to 300 K under an applied magnetic field of 2000 Oe, as shown in Figure 11. The  $\chi_m T$  value per  $\text{Mn}_4\text{Fe}$  at room temperature,  $12.33 \text{ emu K mol}^{-1}$ , is very similar to the spin-only value of  $12.375 \text{ emu K mol}^{-1}$  expected for the magnetically dilute five-spin system ( $S_{\text{Fe}}, S_{\text{Mn}}, S_{\text{Mn}}, S_{\text{Mn}}, S_{\text{Mn}} = (1/2, 2, 2, 2, 2)$ ). When the temperature is lowered,  $\chi_m T$  increases smoothly and then sharply without a minimum to reach a maximum as high as  $41.68 \text{ emu K mol}^{-1}$  at 5.0 K, strongly suggestive of the occurrence of a three-dimensional magnetic ordering. The magnetic susceptibilities obey the Curie–Weiss law with a positive Weiss

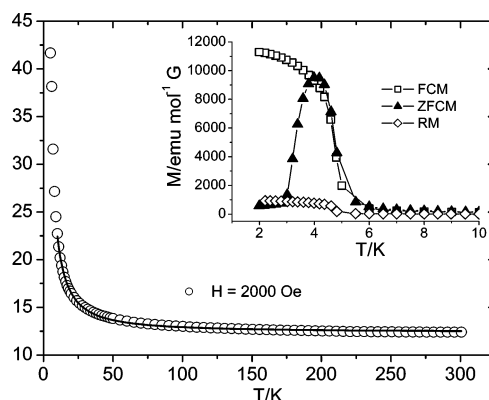


**Figure 11.** Temperature dependence of  $\chi_m T/\text{Mn}_4\text{Fe}$  for complex 7. The solid line represents the calculated values. The inset shows the field-cooled magnetization ( $\square$ ), the zero-field-cooled magnetization ( $\blacktriangle$ ), and the remanent magnetization ( $\diamond$ ) for 7.

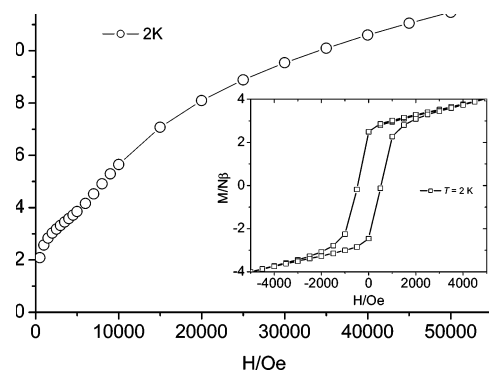


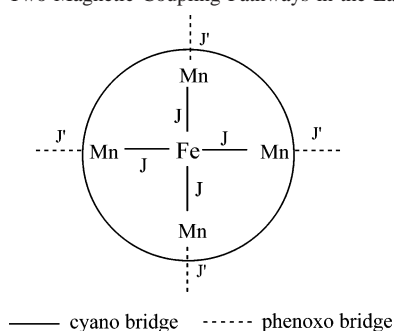
**Figure 12.** Field dependence of magnetization at 2 K for complex 7. The solid lines are guides for the eye. The inset shows the hysteresis loop for 7 at 2 K.

constant  $\theta = 5.64 \text{ K}$  and a Curie constant  $C = 12.1 \text{ emu K mol}^{-1}$ , indicating an overall ferromagnetic interaction between Mn(III) ions and Fe(III) ions through bridging cyanide groups.

To confirm the magnetic phase transition, the FCM and ZFCM curve was measured using the usual procedure. An abrupt increase in the magnetization is observed at  $\sim 4.8 \text{ K}$ , where the remanent magnetization vanishes (inset of Figure 11). These characteristics indicate that complex 7 exhibits a long-range ferromagnetic ordering at 4.8 K. This  $T_c$  value is comparable to that (4.5 K) of the isostructural  $[\text{Mn}(\text{saltmen})]_4[\text{Fe}(\text{CN})_6]\text{ClO}_4$ .<sup>29b</sup>

The magnetization curve at 2 K (Figure 12) shows a rapid increase in  $M$  at low magnetic field, typical of a ferromagnet. At 50 kOe, the magnetization value is  $\sim 12 N\beta$ , lower than the theoretical value of  $17 N\beta$  for a ferromagnetically coupled  $\text{Mn}_4\text{Fe}$  system. Once again, the zfs effect of Mn(III) should account for this phenomenon. Hysteresis at 2 K is evident with the coercive field of about 500 Oe and the remanent magnetization of  $2.5 N\beta$  (inset of Figure 12). These data suggest that complex 7 is a soft ferromagnet.

To evaluate the magnitude of the intramolecular magnetic coupling, we tried to fit the magnetic susceptibilities with an approximate model. The structural data show that in complex 7 there are two different magnetic coupling pathways, cyano bridges and phenoxy bridges. The layers can be schematically illustrated in Scheme 4, where  $J$  is for

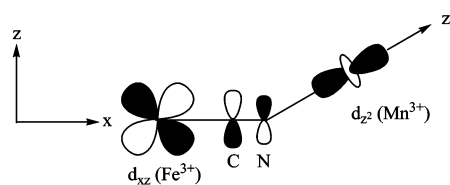
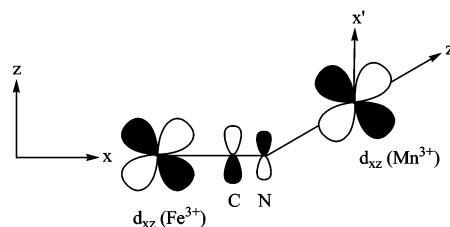
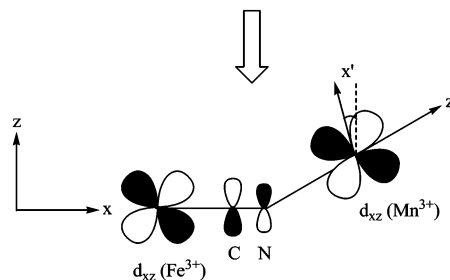
**Scheme 4.** Two Magnetic Coupling Pathways in the Layer of 7

the cyano bridges and  $J'$  for phenoxo ones. It has been reported by Miyasaka et al. that  $|J| \gg |J'|$ ,<sup>29b,29e,29h</sup> and the 2D layer can be therefore described as weakly interacting  $\text{Mn}_4\text{Fe}$  pentanuclear units.

On the basis of above considerations, the magnetic data were fitted to the van Vleck equation for the pentanuclear unit derived from an isotropic exchange Hamiltonian  $\hat{H} = -2J\hat{S}_{\text{Fe}}(\hat{S}_{\text{Mn1}} + \hat{S}_{\text{Mn2}} + \hat{S}_{\text{Mn3}} + \hat{S}_{\text{Mn4}})$ .<sup>29c,50</sup> The magnetic coupling via the phenoxo bridges was treated as intermolecular term using the mean-field method. The final molar magnetic susceptibility ( $\chi_m$ ) is in the form of  $\chi_m = \chi_p/[1 - \chi_p(2zJ'/Ng^2\beta^2)]$ , where  $\chi_p$  is for the  $\text{Mn}_4\text{Fe}$  pentanuclear unit,  $J'$  is the coupling constant between the pentanuclear units, and  $z = 4$ , the number of nearest  $\text{Mn}_4\text{Fe}$  neighbors. The best-fit parameters based on the data above 10 K are  $J = 2.34 \text{ cm}^{-1}$ ,  $zJ' = 0.036 \text{ cm}^{-1}$ ,  $g_{\text{Mn}} = 1.99$ , and  $g_{\text{Fe}} = 2.04$ . The calculated solid line shown in Figure 11 agrees well with the experimental values. The calculated  $J$  value is comparable to that ( $1.4 \text{ cm}^{-1}$ ) for the pentanuclear compound  $[\text{Mn}(\text{salpn})(\text{CH}_3\text{OH})_4][\text{Fe}(\text{CN})_6]\text{ClO}_4 \cdot 9\text{H}_2\text{O}$  ( $\text{salpn}^{2-} = N, N'$ -propylenebis(salicylideneiminato) dianion) reported by Liao et al.<sup>50</sup> The positive  $J'$  value suggests the presence of ferromagnetic  $\text{Mn(III)}-\text{Mn(III)}$  coupling through the phenoxo bridges.

It is noteworthy that the  $\phi$  values for the present complexes cover a wide range ( $11.6-44.3^\circ$ ), which should affect the electronic configuration of  $\text{Fe(III)}$  in  $[\text{Fe}(\text{1-CH}_3\text{im})(\text{CN})_5]^{2-}$ .<sup>45d</sup> When  $\phi$  is equal to  $45^\circ$ , the  $d_{xz}$  and  $d_{yz}$  orbitals are degenerate, whereas other angles cause  $d_{xz}$  to be a little higher in energy if the  $xz$  plane is used to evaluate the  $\phi$  value (Scheme 3). For the present  $[\text{Fe}(\text{1-CH}_3\text{im})(\text{CN})_5]^{2-}$  complexes, the electronic configuration of low-spin  $\text{Fe(III)}$  is unambiguously  $d_{xy}^2d_{yz}^2d_{xz}$ , which is different from that in  $[\text{Fe}(\text{CN})_6]^{3-}$ . In the case of octahedral  $[\text{Fe}(\text{CN})_6]^{3-}$ , the  $d_{xy}d_{yz}d_{xz}$  orbitals are degenerate, and the unpaired electron is equally populated on the three orbitals.

Most cyanide-bridged  $\text{Mn(III)}-\text{Fe(III)}$  complexes reported previously exhibit ferromagnetic interactions with few exceptions. This work affords five more ferromagnetically coupled examples, further revealing that ferromagnetic  $\text{Mn}^{\text{III}}-\text{Fe}^{\text{III}}$  coupling is more usual. This fact seems to be contrary to the predictions according to the strict orbital orthogonality theory because of the presence of magnetic orbital overlap between  $t_{2g}$  orbitals ( $d_{xy}d_{yz}d_{xz}$ ) of high-spin  $\text{Mn(III)}$  and low-spin  $\text{Fe(III)}$  ( $d_{xz}$ ). However, the frequent bending of the  $\text{Mn}-\text{N}\equiv\text{C}-\text{Fe}$  linkages and the rotation of the  $x$  and  $z$  axes for  $\text{Mn(III)}$  compared with the  $xz$  plane for

Situation 1:  $d_{xz}$ - $d_{xz}$  orbital overlap of two metal ions.Situation 2: dihedral angle is zero favoring  $d_{xz}$ - $d_{xz}$  orbital overlap of two metal ions.Situation 3: dihedral angle is nonzero unfavoring  $d_{xz}$ - $d_{xz}$  orbital overlap of two metal ions.**Figure 13.** Different magnetic exchange situations with bent  $\text{Fe}-\text{C}\equiv\text{N}-\text{Mn}$  linkages.

$\text{Fe(III)}$  should reduce the overlap and therefore weaken the antiferromagnetic contribution according to Goodenough-Kanamori rules (Figure 13).<sup>29b,53</sup> Consequently, overall ferromagnetic coupling occurs in complexes **1-5** and **7**. For antiferromagnetically coupled complex **6**, the bending of the bridging linkages and the rotation of the  $xz$  plane for  $\text{Mn(III)}$  are present. However, the smallest  $\text{Mn}-\text{N}\equiv\text{C}$  bond angle in **6** may be responsible for the AF behavior. In addition to the reduction of antiferromagnetic coupling, the bent  $\text{Mn}-\text{N}\equiv\text{C}$  bond angle is unfavorable for the ferromagnetic coupling between  $d_{z^2}$  of  $\text{Mn(III)}$  and  $d_{xz}$  of  $\text{Fe(III)}$  (situation 1 in Figure 13), and below a certain bond angle the overall magnetic coupling becomes antiferromagnetic.

## Conclusions

We first investigated the  $[\text{Fe}(\text{1-CH}_3\text{im})(\text{CN})_5]^{2-}$  building block for the construction of polynuclear or polymeric bimetallic  $\text{Mn(III)}-\text{Fe(III)}$  complexes. The ferromagnetic or antiferromagnetic  $\text{Mn(III)}-\text{Fe(III)}$  coupling has been attributed to the bending of the  $\text{Mn}-\text{N}\equiv\text{C}-\text{Fe}$  linkage and the nonplanarity of the  $xz$  planes of  $\text{Mn(III)}$  and  $\text{Fe(III)}$ . Future work involves the synthesis of cyanide-bridged  $\text{M(II)}-\text{Fe(III)}$  complexes ( $\text{M} = \text{Mn, Ni, Cu}$ ) using the versatile  $[\text{Fe}(\text{1-CH}_3\text{im})(\text{CN})_5]^{2-}$  building block to gain a magnetostructural correlation.<sup>54</sup>

(53) Goodenough, J. B. *Phys. Rev.* **1955**, *100*, 564. Kanamori, J. *J. Phys. Chem. Solids* **1959**, *10*, 87.

(54) Zhang, Y.-Q.; Luo, C.-L.; Yu, Z. *New J. Chem.* **2005**, *29*, 1285.

**Acknowledgment.** This work was supported by the Ministry of Science Technology, China through the 973-project (2002CB613301) and the Fok Ying Tong Education Foundation.

**Supporting Information Available:** Crystallographic data in CIF format, selected bond distances and angles for complex **3**,

structures for complexes **3**, **5**, and **7**, field dependence of magnetization for complexes **1–5**, magnetic fit equations for trinuclear  $Mn_2Fe$  systems, and temperature dependence of AC magnetic susceptibility at zero DC magnetic field. This material is available free of charge via the Internet at <http://pubs.acs.org>.

IC060575I